

Design and Analysis of Junctionless VTFET Device for Sensing Applications

Anwesh¹, Divakaran S.¹, Ravi Prakash Dwivedi¹, Yogendra Singh², Lucky Agarwal^{1,*}

¹ School of Electronics Engineering, Vellore Institute of Technology, Chennai, 600127, India

² IMD, Ministry of Earth Science, Shivaji Nagar Pune, 400050, India

(Received 29 March 2021; revised manuscript received 23 June 2022; published online 30 June 2022)

A dielectric modulation strategy of a TFET structure is reported in this work to improve sensing of biomolecules. A junctionless TFET structure is proposed in order to make the fabrication process easier. Metals with specific work functions are deposited on the source and drain regions to accumulate charge carriers and create the junction. A high- k gate dielectric material (HfO_2) is used to improve the gate capacitance. The performance parameters of the device are given by the OFF-state to ON-state current ratio ($I_{\text{OFF}}/I_{\text{ON}}$) and sub-threshold swing (SS). Further, the structure is made vertical to enhance the electric field so that I_{ON} current will increase up to 10^{-4} A/ μm . A nanocavity near the fixed gate is made to improve the capture area of the biosensor. TCAD models are simulated for the sensitivity range by filling the biosensor neutral/charged biomolecules with different dielectric constants. Due to the joint introduction of vertical and lateral tunnelling, the sensitivity of the proposed biosensor increased to 10^8 . The drain current increased with an increase in the positive charge and decreased with an increase in the negative charge of biomolecules. The sensitivity in the proposed structure increased by a factor of 10^4 compared to the sensitivity reported till date in the literature. This shows that the proposed biosensor can be integrated with solid state circuit to be used in wearable electronics.

Keywords: TFET, Biosensor, Junctionless, Subthreshold swing.

DOI: [10.21272/jnep.14\(3\).03019](https://doi.org/10.21272/jnep.14(3).03019)

PACS number: 87.85.fk

1. INTRODUCTION

Scaling of MOSFET over the years has resulted undesirable surge in short-channel effects such as high on current (I_{on}), $I_{\text{on}}/I_{\text{off}}$ ratio, Drain Induced Barrier Lowering (DIBL), and the subthreshold swing is also restricted to maximum of 60 mV/dec, which limits supply voltage scaling and degrades the device performance. As a result, substantial research is being carried out to replace the devices [1]. To overcome these challenges, the tunnelling field effect transistor (TFET) is used as an effective alternative in which the current conduction happens through band-to-band tunnelling (BTBT) mechanism [2]. When compared to MOSFET, TFET has a substantially lower subthreshold swing. Due to its large tunnelling barrier in the off state, it has a lower leakage current, less power dissipation, and a very less I_{OFF} current [3-5].

A DM-FET based biosensor is an emerging device for its potential to detect biomolecules. This has a number of advantages including downsizing and improved responsiveness with increased sensitivity [6]. Despite its benefits, FETs have a lower sensitivity in the presence of biomolecules. This makes the device less effective in recognizing the biomolecule with good accuracy [7].

In today's era, TFETs are becoming as popular device for medical healthcare among the aging population. The successful prediction of extent of disease contamination and early syndrome finding is important for monitoring the health of patients. Biomolecules such as biotin-streptavidin ($k = 2$) [8], charged amino acid like Gluten ($k = 11-20$); keratin and zein ($k = 5-8$) are necessary to identify the presence of certain diseases [9]. The claimed sensitivity and $I_{\text{on}}/I_{\text{off}}$ ratio, on the other hand, are both extremely low. [10].

The working principle of TFET based biosensor is the development of nanocavity below the gate dielectric of the DM-TFET structure [11]. Nanocavity is formed by etching off a part of the gate dielectric material. The TFET structure detects target biomolecules that are trapped in the nanogap cavity based on changes in the nanogap's dielectric constant, which are then reflected in the drain current [12]. Proteins are simulated with almost the same dielectric constant as the biomolecule. [13, 14]. The diffusion of carriers from the source to the channel area and vice versa complicates the creation of an abrupt junction profile. However, the strong doping of the Source and Drain regions of the TFET structure complicates device fabrication [15].

The above discussed limitation can be overcome by the proposed Junctionless VTFET structure. The junctionless VTFET is a uniformly doped silicon structure in which junctions are formed by charge-plasma concept [16, 17]. The main emphasis in this paper is to improve the I_{ON} current and the sensing property. Simulation is done with different dielectric constants $k = 1, 5, 7$ and 8 for different biomolecules [18]. The effect on sensitivity due to charged and neutral biomolecule is studied. Further, the proposed structure is benchmarked for sensitivity analysis against the structure reported in literature [19, 20].

2. DEVICE STRUCTURE AND THEORY

As demonstrated in Fig. 1b, the nanogaps are generated by etching off both sides of dielectric HfO_2 . The biomolecules capture area is increased by the presence of these nanogaps on both sides of HfO_2 . The biomolecules are anchored by a layer with a thickness of 5 nm. The simulation is run using the VTFET as biosensor.

* ravieciit@gmail.com

The results were presented at the 2nd International Conference on Innovative Research in Renewable Energy Technologies (IRRET-2022)

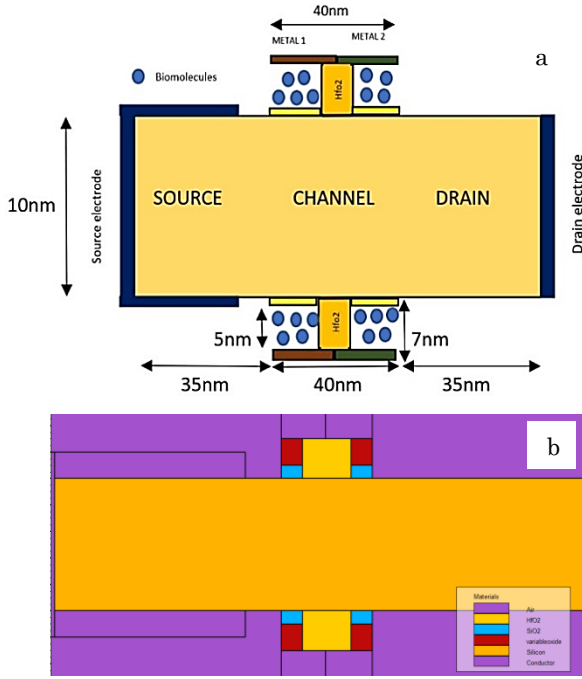


Fig. 1 – (a): Schematic of the nanogap embedded JL VTFET device and (b): Cross sectional device structure of Junctionless Vertical TFET

Fig. 1a depicts the proposed Junctionless $I_{\text{off},k}$ and $I_{\text{off,Air}}$ are the drain currents when nanogaps are filled with biomolecules and when it is empty at fixed V_{GS} and V_{DS} . It is seen from the Fig. 2 that with increase in value of K , there is decrease in I_{off} current and hence sensitivity increases. JL VTFET has sensitivity in order of 10^6 when $k = 8$. More Electric field lines can be generated by increasing the k value that decreases the off current and increases the I_{on} . The device’s gate is divided into two sections, with work functions $\Phi_{m1} = 5.4 \text{ eV}$ and $\Phi_{m2} = 5.9 \text{ eV}$ that is near to source and drain sides respectively. The length of gate from source to drain is 40 nm. The device has a doping concentration of $1 \times 10^{19} \text{ cm}^{-3}$.

Silvaco TCAD programme. Only one type of biomolecule is thought to be anchored at a time within the cavities. The simulation looks at neutrally charged biomolecules, negatively charged biomolecules, and positively charged biomolecules. Various mathematical models are adapted to analyze the device.

3. RESULTS AND DISCUSSION

This section discusses the simulation results of the proposed Junctionless VTFET based biosensor considering four dielectric constants ($k = 1, 2, 5, 8$). Impact of charged biomolecules in on current (I_{on}) is taken into consideration.

3.1 Changes in Sensitivity Due to Neutral Biomolecules

Fig. 2 shows the change in drain current with gate voltage (V_{GS}) for JL VTFET for neutral biomolecules having $k = 1$ at $V_{\text{DS}} = 1 \text{ V}$ for completely filled nanogaps. When $k = 1$, the nanogap cavity is filled with air. The diagram depicts that as the dielectric constant

increases, the I_{on} current increases. In addition to lateral tunnelling, band-to-band tunnelling occurs perpendicular to the gate oxide. Additionally, using a gate metal with a larger work function near the drain, decreases the OFF-state current (I_{off}). I_{OFF} is mostly determined by thermionic emission as with the MOSFET rather than tunnelling probability. This also helps with the SS improvement. As a result, the overall I - V characteristics is improved. The sensitivity of these biosensors when immobilized with neutral biomolecules is investigated. Due to its capacity to reflect the sensor's reaction to the detecting targets, the condition when the nanogap is empty or filled with air is chosen as a reference for biosensors. The sensitivity of the device is calculated by [19].

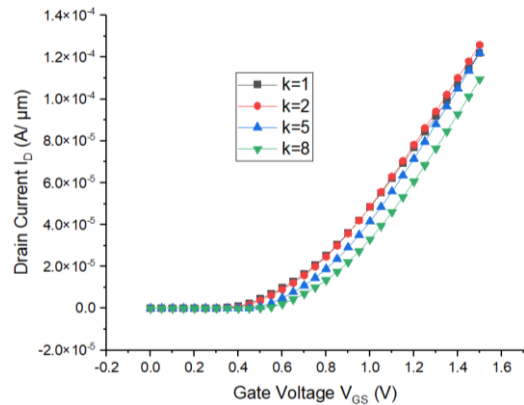


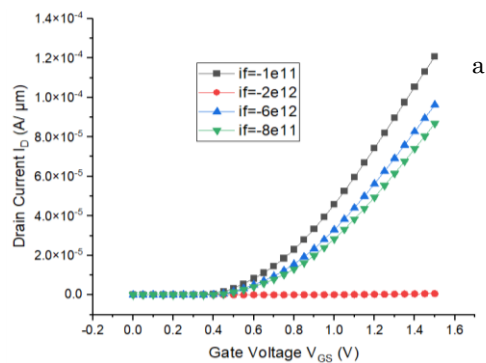
Fig. 2 – I - V curve for neutral biomolecules at $k = 1, 2, 5,$ and 8

$$Sensitivity(S_n) = \frac{I_{\text{Doff,Air}}}{I_{\text{Doff},k}} \bigg|_{V_{\text{GS}}, V_{\text{DS}}} \quad (1)$$

3.2 Impact of Charged Biomolecules

Fig. 3 and Fig. 4 illustrate the effect of charged biomolecule on drain current at fixed V_{GS} for JL VTFET with $k = 1, 2, 5, 8$. The drain current rises with the increase in positive charge and decreases with increase in negative charge of biomolecule per unit area. This is because when positive charge biomolecule fills the nanogaps, the biosensor's surface potential drops. The next sub-sections give the details of impact of charged biomolecules.

1) Change in Sensitivity due to Negative Charge Biomolecules



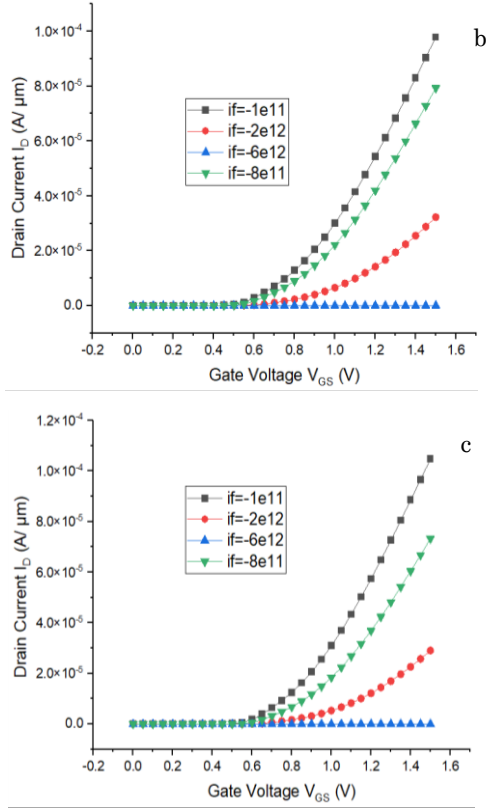


Fig. 3 – Change in I - V characteristics for negatively charged biomolecule at $k = 2$ (a), $k = 5$ (b) and $k = 8$ (c)

The graphs show that with increase in the amount of negatively charged biomolecules, the sensitivity decreases. The potential balance equation of the metal-oxide semiconductor is given by [19]

$$V_{GS} = \Psi_s + \Phi_{MS} - \left(\frac{q \pm N}{C_{eff}} \right) \quad (2)$$

where Ψ_s represents the surface potential, N denotes the charge of biomolecule per unit area, Φ_{ms} represents the contact potential, C_{eff} represents the effective capacitance per unit area and q is unit charge. If V_{GS} and K are fixed the value of negative charged biomolecule is increased, then Ψ_s decreases which causes decrease in the drain current and hence decreases sensitivity. Furthermore, raising the value of k while maintaining V_{GS} and N as constant leads to rise in Ψ_s and results in increase of drain current and therefore sensitivity.

2) Change in Sensitivity due to Positive Charge Biomolecules

The influence of positive charge biomolecules on I - V characteristics and sensitivity is studied in this section. Fig. 4a, b, c shows the change in drain current in presence of positive charge biomolecule at $k = 2, 5, 8$. Similar to section 1, there is an increasing slope in the plots. Positive charged biomolecules at the interface region reduces the p -type channel, allowing for enhanced tunnelling at the source to channel junction. This explains scaling down of threshold voltage and reduction in V_{GS} required for operation of the device.

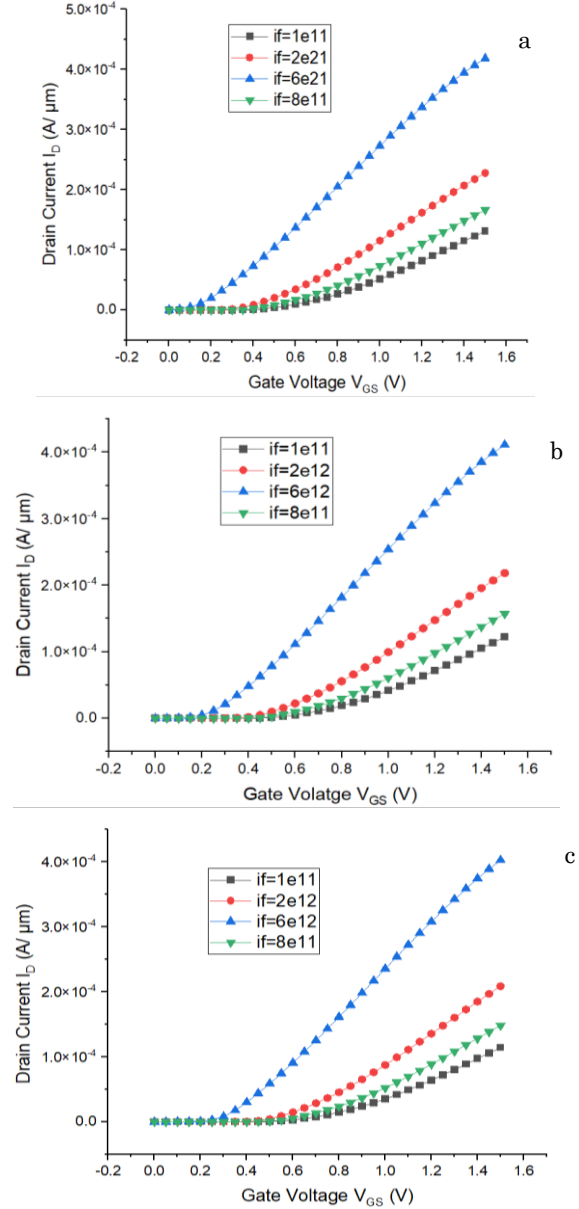


Fig. 4 – Change in I - V characteristics for positive charge biomolecule at $k = 2$ (a), $k = 5$ (b), $k = 8$ (c)

Table 1 – Extracted value of proposed structure for $k = 8$

Reported works	SS (mV/dec)	I_{on}/I_{off} ratio	Sensitivity
DG-TFET [16]	50	5.8×10^2	1.05×10^2
Conventional TFET [17]	50.6	–	50
Lateral DMFET [20]	74	10^1	10
Vertical DMFET [20]	64	10^2	40
Proposed structure	45.8	1.38×10^{10}	6.756×10^4

Table 1 shows the values of short channel parameters of the proposed structure at $k = 8$ in presence of charged biomolecules. Change in the interface charge alters the short channel parameters. Increase in positive interface charge creates reduction in the I_{OFF} current with a lower threshold voltage compared to the

previous smaller positive interface charge. We can observe from Table 1 that reduction in the sub threshold swing happens with increase in positive interface charge. In the same way, increase in the negative interface charge creates decrease in I_{on} and I_{off} current and a higher threshold voltage compared to the previous smaller negative interface charge. We can observe from Table 1 that decrease in negative interface charge reduces the V_{TH} with slight increase in sub threshold

Table 2 – Comparison of the proposed structure with reported biosensor

Interface Charge	I_{off} (A/ μ m)	I_{on} (A/ μ m)	V_{TH} (V)	Sub-threshold swing (mV/decade)	Sensitivity
0.00	7.88×10^{-15}	1.09×10^{-5}	3.40×10^{-1}	4.58×10^1	2.09×10^3
1.00×10^{11}	9.70×10^{-15}	1.14×10^{-4}	3.36×10^{-1}	4.59×10^1	1.70×10^3
4.00×10^{11}	1.82×10^{-14}	1.28×10^{-4}	3.02×10^{-1}	4.61×10^1	9.07×10^2
8.00×10^{11}	4.37×10^{-14}	1.48×10^{-4}	2.62×10^{-1}	4.64×10^1	3.78×10^2
2.00×10^{12}	6.42×10^{-13}	2.08×10^{-4}	1.53×10^{-1}	4.76×10^1	2.57×10^1
6.00×10^{12}	2.29×10^{-9}	4.00×10^{-4}	1.32×10^{-1}	4.91×10^1	7.20×10^3
-6.00×10^{12}	9.15×10^{-18}	8.41×10^{-17}	6.54×10^{-1}	4.81×10^1	1.80×10^8
-2.00×10^{12}	2.44×10^{-16}	2.90×10^{-5}	5.58×10^{-1}	4.68×10^1	6.76×10^4
-8.00×10^{11}	1.65×10^{-15}	7.82×10^{-5}	4.35×10^{-1}	4.71×10^1	1.00×10^4

REFERENCES

1. A. Goel, S. Rewari, S. Verma, S.S. Deswal, R.S. Gupta, *IEEE Sensor. J.* **21** No 15, 16731 (2021).
2. N. Paras, S.S. Chauhan, *International Conference on Advances in Computing and Communication Engineering* (ICACCE-2019).
3. W.C. Ma, *IEEE T. Electron Dev.* **64** No 3, 1390 (2017).
4. A. Goel, S. Rewari, S. Verma, R.S. Gupta, *IEEE Electron Devices Kolkata Conference* (EDKCON-2018).
5. Y. Lu, G. Zhou, L. Rui, L. Qingmin, Q. Zhang, T. Vasen, S.D. Chae, *IEEE Electron Dev. Lett.* **33** No 5, 655 (2012).
6. M. Abdullah-Al-Kaiser, D.J. Paul, Q.D.M. Khosru, *IEEE Region 10 Humanitarian Technology Conference* (R10-HTC-2017).
7. L. Lin, C. Li, Z. Zhang, E. Alexov, *J. Chem. Theory Comput.* **9** No 4, 2126 (2013).
8. F. Bibi, M. Villain, C. Guillaume, B. Sorli, N. Gontard, *Sensors* **16** No 8 1232 (2016).
9. S. Busse, V. Scheumann, B. Menges, S. Mittler, *Biosens. Bioelectron.* **17**, 704 (2002).
10. G. Joshi, N. Sood, I. Saini, *3rd International Conference on Electronics, Communication and Aerospace Technology* (ICECA-2019).
11. Q. Huang, R. Huang, W. Chunlei, Hao Zhu, C. Chen, J. Wang, L. Guo, *IEEE International Electron Devices Meeting* (IEEE-2014).
12. M. Chanda, R. Das, A. Kundu, C.K. Sarkar, *Superlattice. Microst.* **104**, 451 (2017).
13. D. Sharma, D. Singh, S. Pandey, S. Yadav, P.N. Kondekar, *Superlattice. Microst.* **111**, 767 (2017).
14. S. Sahoo, S. Dash, G.P. Mishra, *Devices for Integrated Circuit* (DevIC, IEEE-2019:2019).
15. K. Chang-Hoon, J. Cheulhee, H.G. Park, Y. Choi, *Biochip J.* **2** No 2, 127 (2008).
16. V. Devi, B. Bhowmick, P. Pukhrambam, *IEEE T. Nanotechnol.* **19**, 156 (2020).
17. S. Kumar, Y. Singh, B. Singh, P.K. Tiwari, *IEEE Sensor. J.* **20** No 21, 12565 (2020).
18. M. Anvarifard, K. Mohammad, Z. Ramezani, I. Sadegh Amiri, *IEEE Sensor. J.* **14**, 6880 (2020).
19. R. Goswami, B. Bhowmick, *IEEE Sensor. J.* **19** No 21, 9600 (2019).
20. M. Verma, S. Tirkey, S. Yadav, D. Sharma, D. Singh Yadav, *IEEE T. Electron Dev.* **64**, 3841 (2017).

Проектування та аналіз безперехідного пристрою VTFET для сенсорних додатків

Anwesh¹, Divakaran S.¹, Ravi Prakash Dwivedi¹, Yogendra Singh², Lucky Agarwal¹

¹ School of Electronics Engineering, Vellore Institute of Technology, Chennai, 600127, India

² IMD, Ministry of Earth Science, Shivaji Nagar Pune, 400050, India

У роботі повідомляється про стратегію діелектричної модуляції структури TFET для покращення зондування біомолекул. Безперехідна структура TFET запропонована для спрощення процесу виготовлення. Метали з певними роботами виходу електронів осаджуються на ділянках джерела та стоку для накопичення носіїв заряду та створення переходу. Для покращення ємності затвора використовується діелектричний high- k матеріал (HfO₂). Експлуатаційні параметри пристрою визначаються співвідношенням струмів у вимкненому стані до увімкненого (I_{OFF}/I_{ON}) і підпороговим коливанням (SS). Далі конструкцію роблять вертикальною для підсилення електричного поля, отже іонний струм збільшується до 10^{-4} А/мкм. Для покращення області захоплення біосенсора зроблена нанопорожнина біля нерухомого затвора. Моделі TCAD моделюються для діапазону чутливості

шляхом заповнення біосенсора нейтральними/зарядженими біомолекулами з різними діелектричними сталими. Завдяки спільному впровадженню вертикального та бічного тунелювання чутливість пропонованого біосенсора зросла до 10^8 . Струм стоку збільшувався зі збільшенням позитивного заряду та зменшувався зі збільшенням негативного заряду біомолекул. Чутливість у запропонованій структурі зросла в 10^4 рази порівняно з чутливістю, про яку повідомлялося в літературі. Це показує, що запропонований біосенсор може бути інтегрований з твердотільною схемою для використання в розумній електроніці.

Ключові слова: TFET, Біосенсор, Безперехідний, Підпорогове коливання.